SUPPLEMENTARY INFORMATION

Modulating the DNA polymerase β reaction equilibrium to dissect the reverse reaction

David D. Shock[1], Bret D. Freudenthal[1,2], William A. Beard[1], and Samuel H. Wilson[1]*

[1]Genome Integrity and Structural Biology Laboratory, National Institute of Environmental Health Sciences, NIH, Research Triangle Park, North Carolina, USA. [2]Department of Biochemistry and Molecular Biology, The University of Kansas Medical Center, Kansas City, Kansas, USA. *e-mail: wilson5@niehs.nih.gov

Supplementary Results

Supplementary Figures

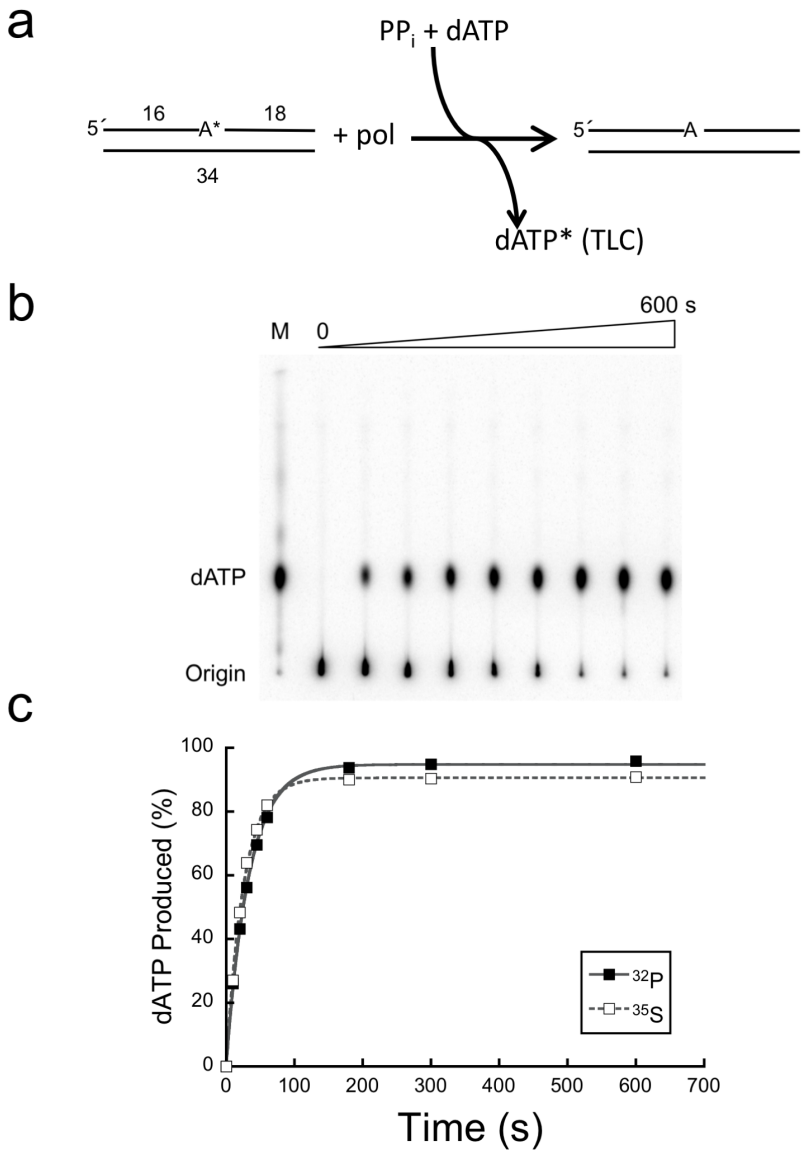

Supplementary Figure 1 | Thio-elemental effect on pyrophosophorolysis. (**a**) Diagram illustrating the assay used to follow pyrophosphorolysis. On a nicked DNA substrate, pol β utilizes PP_i to remove the 3′-[^{32}P]dAMP or 3′-[^{35}S]dAMP (A*) generating [α-^{32}P]dATP or [α-^{35}S]dATP (dATP*), respectively. A cold dATP or dATP(αS) trap was included in the reaction to prevent insertion of the radioactive product and to regenerate nicked DNA with an unlabeled 3′-terminus. Product formation (dATP*) was monitored by TLC. (**b**) Image of the exposed TLC plate for formation of [α-^{32}P]dATP. Lane M is [α-^{32}P]dATP alone. An image of the full plate is shown in **Supplementary Figure 8a.** (**c**) Pol β-dependent dATP* formation in the presence of 1 mM PP_i with a 3′-[^{32}P]dAMP (■) or 3′-[^{35}S]dAMP (□) primer terminus. Single-turnover time courses were fit to a single exponential (solid and dashed gray lines for ^{32}P- and ^{35}S-labeled dATP, respectively) (k_{obs} = 0.030/s and 0.039/s for removal of ^{32}P- and ^{35}S-labeled dAMP, respectively).

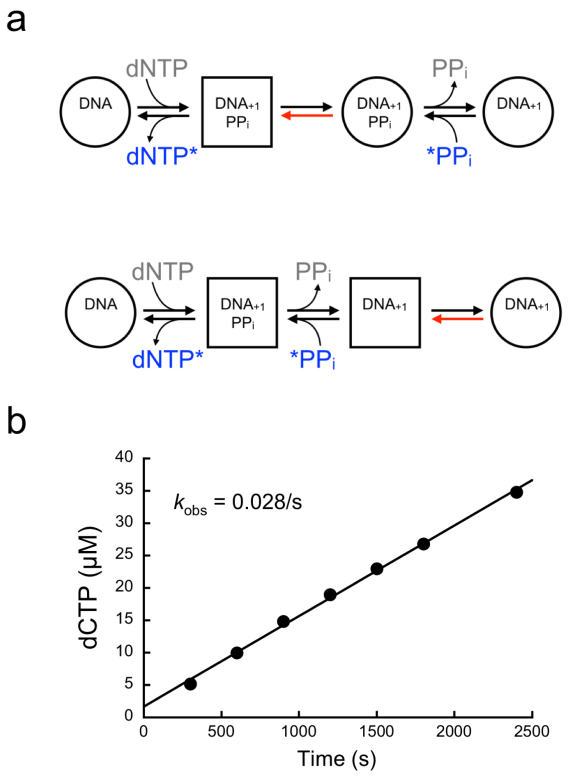

Supplementary Figure 2 | Pyrophosphate exchange. (a) The exchange reaction follows the movement of radioactive-label in [^{32}P]PP$_i$ into dNTP to distinguish whether PP$_i$ binding occurs prior to (upper panel) or following (lower panel) a rate-limiting conformational change (red arrow)[50]. In this experiment, the ternary product complex was generated *in situ* (unlabeled dNTP is present to generate nicked DNA and cold PP$_i$, gray labels) under single-turnover conditions (pol>>DNA) and the rate of radioactive movement from labeled PP$_i$ into dNTP (blue) was measured. These schemes illustrate that if PP$_i$ binding occurs prior to the slow conformational change, then the measured rate of pyrophosphorolysis will be similar to the rate of exchange. In contrast, if PP$_i$ binding occurs *after* the slow conformational change, then the rate of exchange (rapid PP$_i$ binding and chemistry) will be faster than the measured rate of pyrophosphorolysis. **(b)** Pol β was pre-incubated with unlabeled nicked DNA and mixed with a solution containing [^{32}P]PP$_i$ and cold dCTP. Radioactive dCTP was followed by TLC. The solid line represents the best fit to a linear equation. The observed rate for the exchange reaction (slope/enzyme-DNA complex) was 0.028/s. Since the rate of PP$_i$ exchange as determined by substrate cycling (i.e., alternating nucleotide insertion and removal) is similar to that measured by single-turnover analysis, PP$_i$ binding occurs prior to the conformational change. Since the rate of PP$_i$ exchange as determined by substrate cycling (i.e., alternating nucleotide insertion and removal) is similar to that measured by single-turnover analysis, PP$_i$ binding occurs prior to the conformational change.

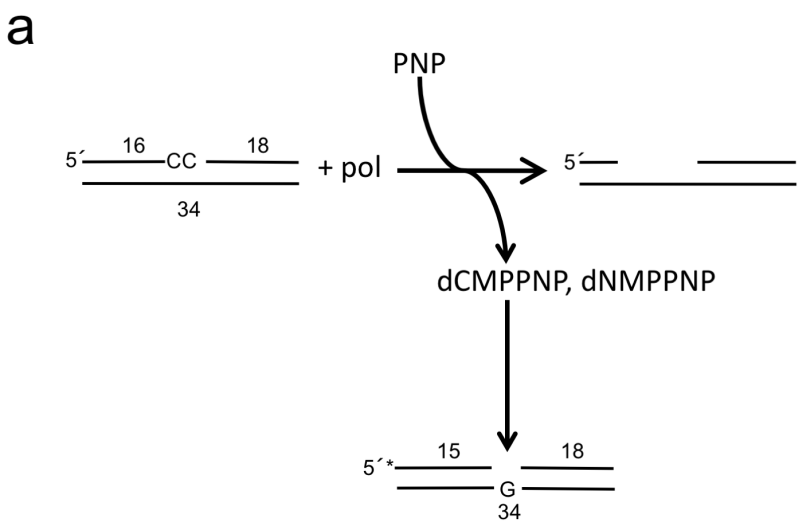

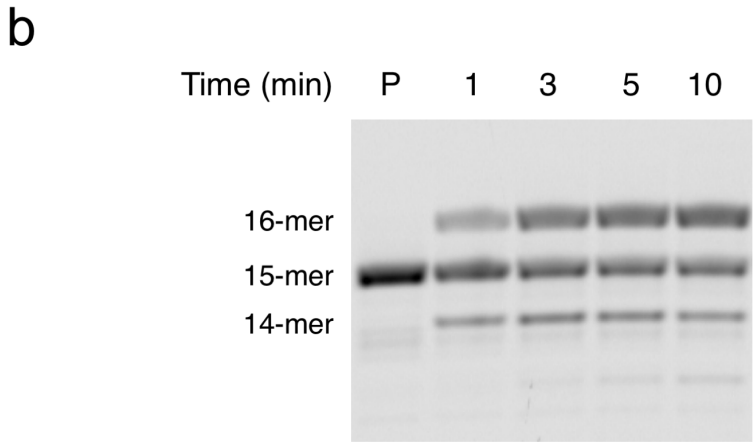

Supplementary Figure 3 | PNP-induced gap-filling reaction. (**a**) Diagram illustrating the assay used to follow PNP-induced gap-filling DNA synthesis. An unlabeled nicked DNA substrate with two deoxycytidine residues at the 3´-primer terminus was incubated with a low concentration of PNP as described in Online Methods. A single-nucleotide gapped DNA substrate (G in the gap) with a 5´-6-FAM (*) 15-mer labeled primer (P) was then mixed with this solution to determine if complementary deoxynucleoside triphosphates (i.e., dCMPPNP) were generated in the initial reaction that could be used to fill the gap. (**b**) Substrate/products were resolved on a denaturing gel and visualized by phosphorimaging. Gap-filling DNA synthesis generates a 16-mer product, while pyrophosphorolysis creates a 14-mer product. An image of the full gel is shown in **Supplementary Figure 8b.**

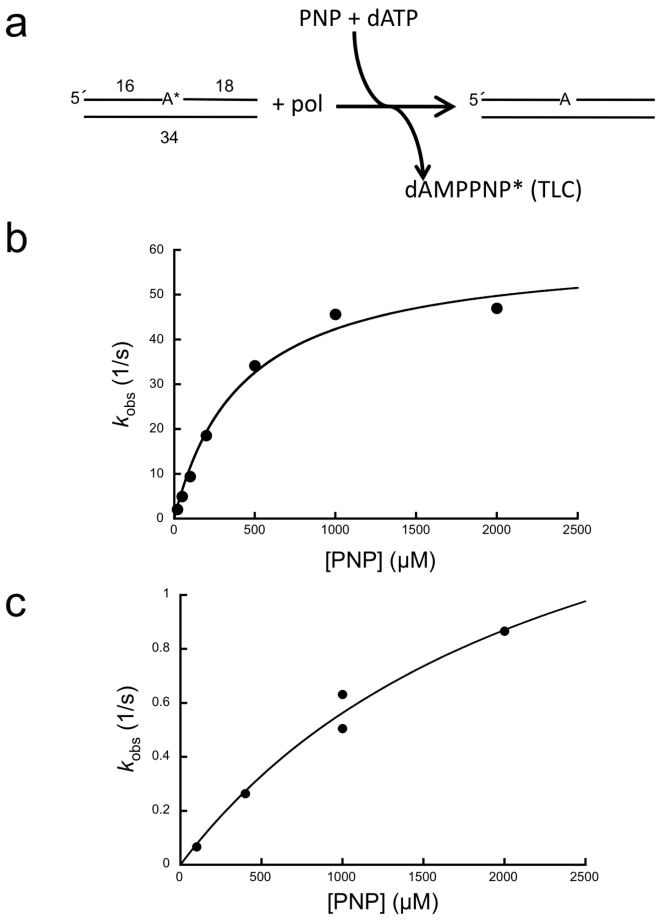

Supplementary Figure 4 | Thio-elemental effect on PNP-dependent reverse reaction. (**a**) Diagram illustrating the assay used to follow PNP-dependent reverse reaction. A nicked DNA substrate utilizes PNP to remove a 3′-[^{32}P]dAMP or 3′-[^{35}S]dAMP (A*) generating [α-^{32}P]dAMPPNP or [α-^{35}S]dAMPPNP (dATP*), respectively. A cold dATP trap was included in the reaction to prevent insertion of the radioactive product and to regenerate nicked DNA with an unlabeled 3′-terminus. Product formation (dATP*) was monitored by TLC. (**b**) A secondary plot of the PNP concentration dependence of the observed first-order rate constants (k_{obs}) for single-turnover time courses for the removal of a 3′-[^{32}P]dAMP in nicked DNA. These data were fit to a hyperbola (Eq. 1, gray line) to derive k_{rev} and K_d (**Supplementary Table 1**). (**c**) A secondary plot of the PNP concentration dependence of the observed first-order rate constants (k_{obs}) for single-turnover time courses for the removal of a 3′-[^{35}S]dAMP in nicked DNA. The duplicate points at 1000 μM PNP represents data from independent experiments. These data were fit to a hyperbola (Eq. 1, gray line) to derive k_{rev} and K_d (**Supplementary Table 1**).

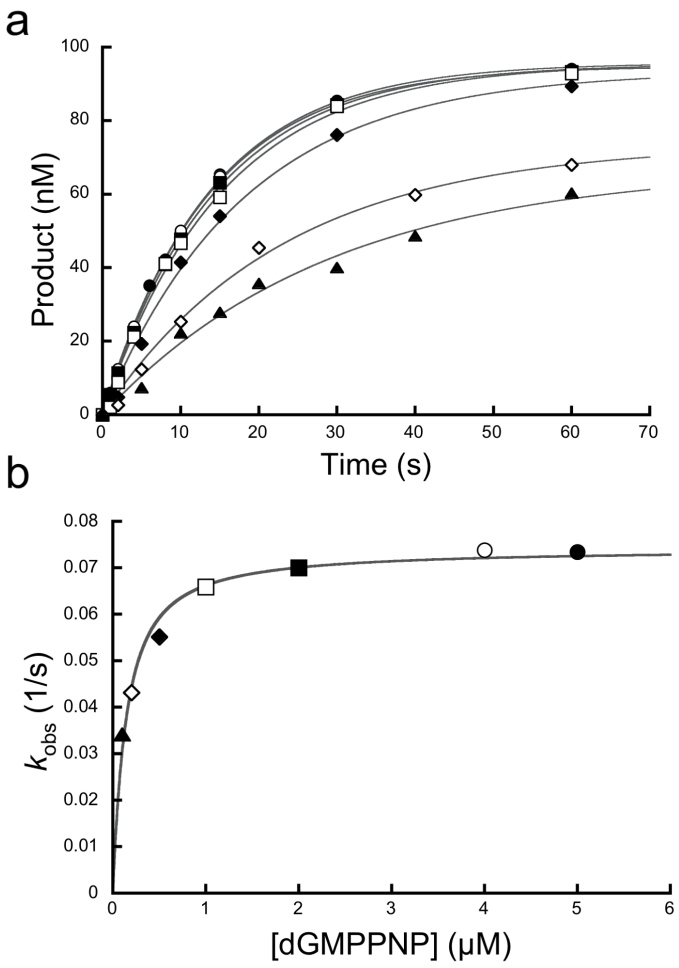

Supplementary Figure 5 | Single-turnover analysis for gap filling insertion with dGMPPNP. (**a**) Pol β-dependent single-nucleotide gap filling DNA synthesis with 0.1 μM (▲), 0.2 μM (◇), 0.5 μM (◆), 1 μM (□), 2 μM (■), 4 μM (❍) and 5 μM (●) dGMPPNP. Time courses were fit to a single exponential (gray lines). (**b**) A secondary plot of the dGMPPNP concentration dependence of the observed first-order rate constants (k_{obs}). These data were fit to a hyperbola (Eq. 1, gray line) to derive k_{pol} and K_d (**Supplementary Table 1**).

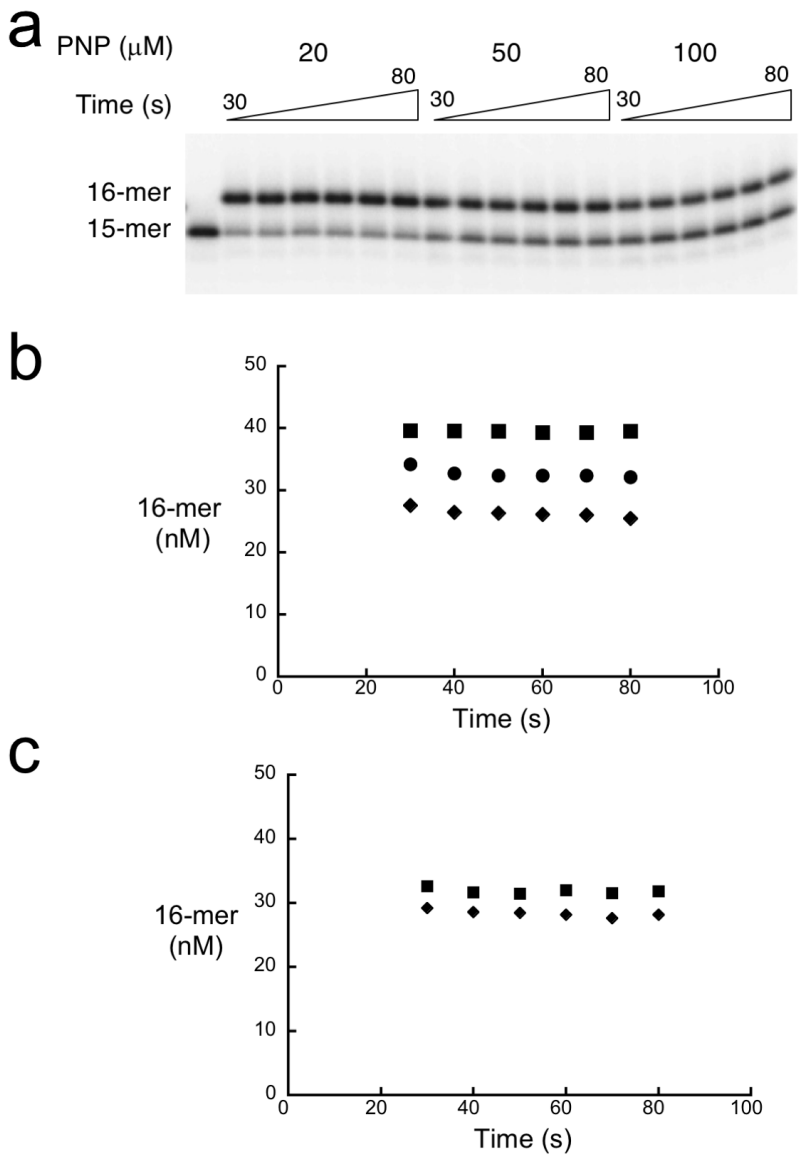

Supplementary Figure 6 | Equilibrium analysis of pol β bound with one-nucleotide gapped and nicked DNA. (**a**) Image of a representative sequencing gel showing the time dependence of single-nucleotide gap filling in the presence of 20, 50 or 100 μM PNP. An image of the full gel is shown in **Supplementary Figure 8c.** In this assay, the 5′-labeled primer (15-mer) can be extended one nucleotide (16-mer). The first lane includes primer only. (**b**) Quantification of the gel shown in panel **a** indicating that equilibrium had been established (i.e., concentration of DNA product does not change with time, 30-80 s) and that the amount of product is sensitive to the concentration of PNP (■, 20 μM; ●, 50 μM; ◆, 100 μM). The calculated equilibrium constants are 1.5, 1.9, and 2.2 for 20, 50 and 100 μM PNP, respectively. (**c**) Quantification of an assay with PP_i indicating that equilibrium had been established and that the amount of product is weakly sensitive to the concentration of PP_i (■, 1000 μM; ◆, 2000 μM). The calculated equilibrium constants are 62,700 and 82,300 for 1000 and 2000 μM PP_i, respectively.

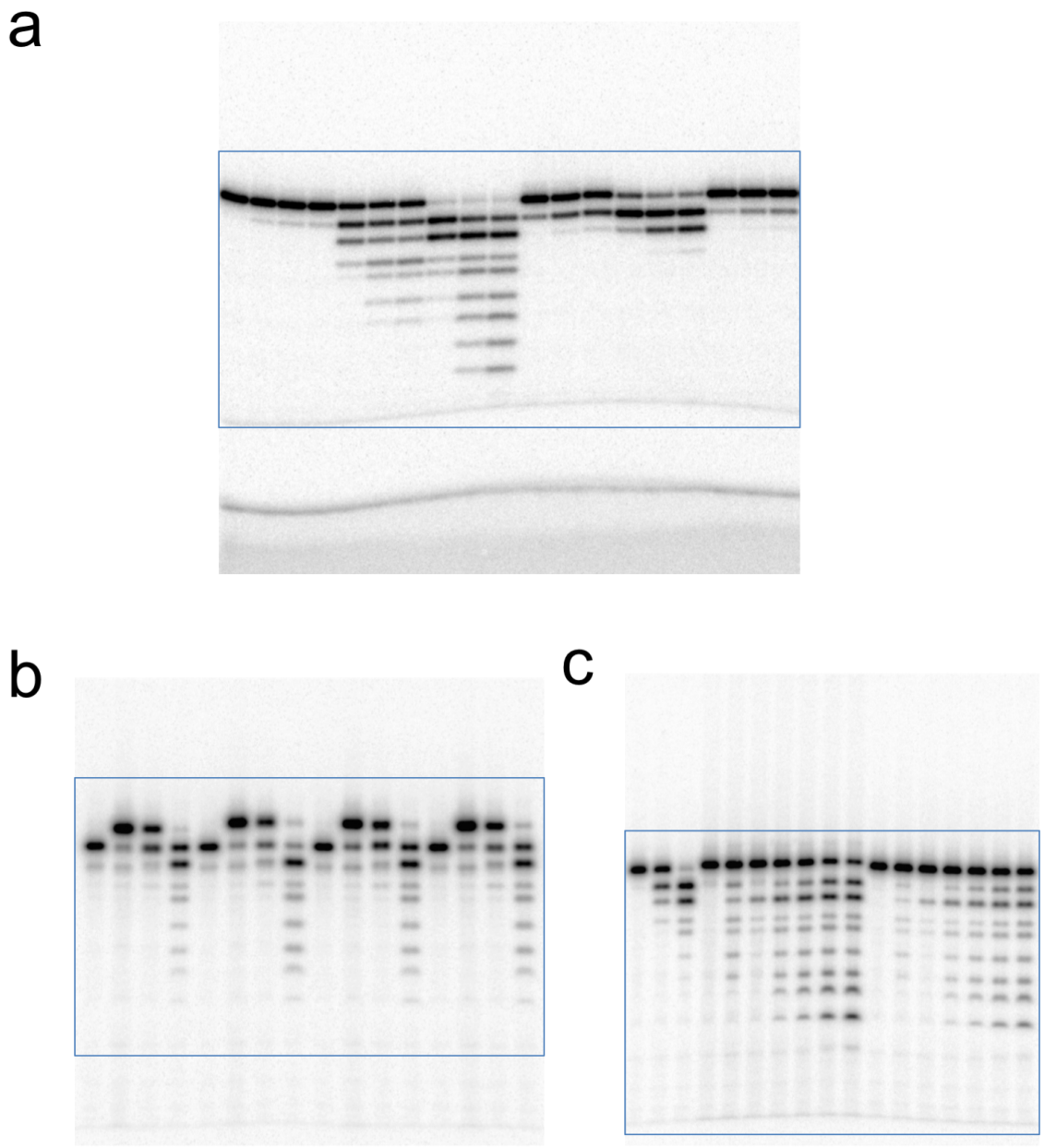

Supplementary Figure 7 | Full gel images. The cropped image in the respective figures is indicated. (**a**) Figure 2. (**b**) Figure 4a. (**c**) Figure 4b.

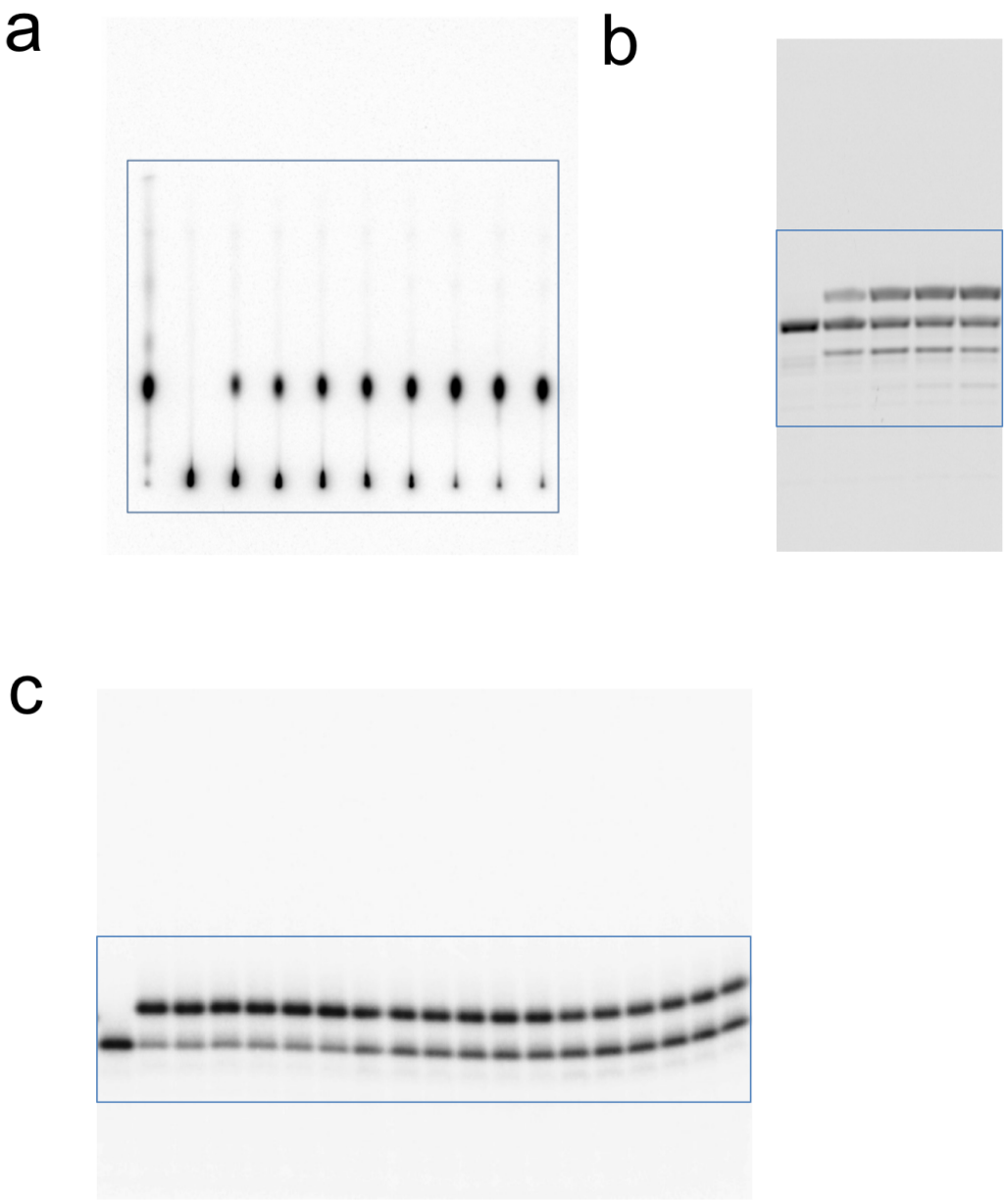

Supplementary Figure 8 | Full TLC plate or gel images. The cropped image in the respective figures is indicated. (**a**) Supplementary Figure 1b. (**b**) Supplementary Figure 3b. (**c**) Supplementary Figure 6a.

Supplementary Tables

Supplementary Table 1. Summary of kinetic parameters[a]

DNA	Ligand	k_{max}[b] (s^{-1})		K_d (μM)		k_{max}/K_d 10^{-4} ($s^{-1}\mu M^{-1}$)	
nicked	PP_i	0.03	(0.0003)	90	(3)	3.33	(0.12)
	PNP	32.6	(1.0)	339	(27)	962	(82)
gapped	dGTP[c]	13.7	(1.3)	1.3	(0.2)	105385	(19048)
	dGMPNPP	0.074	(0.002)	0.12	(0.02)	6167	(1041)

[a]Values (k_{max} and K_d) are best-fit parameters (standard error) of non-linear least-squares fits of secondary plots of the ligand concentration dependence of k_{obs} to a hyperbola, Eq. 1.

[b]Represents k_{rev} and k_{pol} for the reverse and forward (DNA synthesis) reactions. Different steps are rate limiting for the PP_i and PNP dependent reverse reaction. Pyrophosphorolysis is limited by a non-chemical step, whereas the PNP reaction is limited by the chemical step.

[c]Taken from a previous study[23].

Supplementary Table 2. Data collection and refinement statistics

	Nick DNA/PNP Substrate Complex	Reactant Complex	1-nt gap/dCMPPNP Product Complex
Data collection			
Space group	$P2_1$	$P2_1$	$P2_1$
Cell dimensions			
a, *b*, *c* (Å)	50.6,79.3,55.2	50.7,79.9,55.3	50.8,79.9,55.5
α, β, γ (°)	90,107.5,90	90,107.6,90	90,107.7,90
Resolution (Å)	50-1.90	50-2.0	50-1.96
R_{sym} or R_{merge}[a] (%)	7.3 (45.0)	7.4 (50.5)	7.5 (43.6)
$I/\sigma I$	19.8 (2.4)	20.2 (2.2)	18.9 (2.4)
Completeness (%)	99.0 (100)	99.2 (92.4)	99.3 (93.5)
Redundancy	5.0 (2.9)	5.2 (2.7)	4.7 (2.8)
Refinement			
Resolution (Å)	1.90	2.0	1.96
No. reflections	32852	28404	30285
R_{work}/ R_{free}	0.17/0.23	0.18/24	0.17/0.23
No. atoms			
Protein	2662	2675	2673
DNA	659	659	633
Water	376	256	318
B-factors (Å^2)			
Protein	25.2	32.2	29.5
DNA/PNP/dCMPPNP	27.1/26.1/-	39.7/35.3/27.5	36.4/-/17.2
$Water_{bulk}$/$water_{bridge}$[b]	31.1/-	36/35.1	33.5/19.6
R.m.s deviations			
Bond length (Å)	0.007	0.007	0.01
Bond angles (°)	1.05	1.2	1.1
Reaction Ratio			
RS/PS occupancy[c]	1.0/0	60/40	0/1.0
PNP	0.7	0.40	0
dCMPPNP	0	0.60	1.0

[a]Highest resolution shell is shown in parentheses.
[b]$Water_{bulk}$ and $water_{bridge}$ refers to the bulk water and Arg183 bridging water respectively.
[c]RS and PS refer to the reactant- and product-state, respectively.

Supplementary References

50. Gabbara, S., and Peliska, J.A. (1996) Catalaytic activities associated with retroviral and viral polymerases. *Methods Enzymol.* **275**, 276-310.